Experimental Realization of an Information Machine with Tunable Temporal Correlations

Tamir Admon,[1] Saar Rahav,[2,*] and Yael Roichman[1,†]
[1]Raymond & Beverly Sackler School of Chemistry, Tel Aviv University, Tel Aviv 6997801, Israel
[2]Schulich Faculty of Chemistry, Technion—Israel Institute of Technology, Haifa 3200008, Israel

(Received 10 July 2018; revised manuscript received 20 September 2018; published 1 November 2018)

We experimentally realize a Maxwell's demon that converts information gained by measurements to work. Our setup is composed of a colloidal particle in a channel filled with a flowing fluid. A barrier made by light prevents the particle from being carried away by the flow. The colloidal particle then performs biased Brownian motion in the vicinity of the barrier. The particle's position is measured periodically. When the particle is found to be far enough from the barrier, feedback is applied by moving the barrier upstream while maintaining a given minimal distance from the particle. At steady state, the net effect of this measurement and feedback loop is to steer the particle upstream while applying very little direct work on it. This clean example of a Maxwell's demon is also naturally operated in a parameter regime where correlations between outcomes of consecutive measurements are important. Interestingly, we find a tradeoff between output power and efficiency. The efficiency is maximal at quasistatic operating conditions, whereas both the power output and rate of information gain are maximal for very frequent measurements.

DOI: 10.1103/PhysRevLett.121.180601

Can a heat engine extract work from a single heat bath? Can a particle be driven against a fluid flow without being pushed by an external force? In his celebrated thought experiment, James Clerk Maxwell presented an example demonstrating that the observation of microscopic details makes such processes possible [1,2]. In 1929, Leó Szilárd quantified the connection between information and thermodynamics by constructing a simple model of an information engine [3]. Szilárd imagined a partition that is inserted into a vessel containing one gas particle. A measurement is then used to determine in which half of the vessel the particle is located, and this information is used to extract work out of the system via an isothermal expansion process. Crucially, Szilárd found that the amount of work extracted by the engine in each cycle is proportional to the information gained by measuring the particle's position, quantified by the Shannon entropy [4] of outcome probabilities $S = k_B I = -k_b \sum_i p_i \ln p_i = k_B \ln 2$. (For $p_R = p_L = 1/2$.)

What was conceived as a thought experiment is now a reality. Theoretical and technological advances have generated new interest in the deep connection between the manipulation of information and thermodynamics. An extensive research effort has led to the development of fluctuation theorems for processes with feedback [5–8], investigation of Landauer's principle [9,10], as well as several other aspects of the thermodynamics of information [9,11–15]. Much of the recent progress in the field is summarized in the review of Parrondo, Horowitz, and Sagawa [16]. One important result with relevance for information engines is a version of the second law of thermodynamics for processes with measurements and feedback [5–8],

$$\langle W \rangle \geq \Delta F - k_{\mathrm{B}} T \langle I \rangle. \tag{1}$$

Here, $\langle W \rangle$ is the (ensemble averaged) work done on the system, ΔF is a free-energy difference, and $\langle I \rangle = \sum_{x,m} p(x,m) \ln[p(x,m)/p(x)p(m)]$ is the mutual information between the measurement outcome m and the state of the system x. This version of the second law shows that additional work can be extracted from processes with positive $\langle I \rangle$. Both this generalization of the second law and the fluctuation theorems it is derived from were studied in several recent experiments [9,11,13,17].

Information engines were realized experimentally in a variety of systems, such as quantum dots, colloidal particles, microwave cavities, and more. In many of these realizations, the time between measurements is very long, so that the engine's behavior at a driving cycle does not depend on what it did in previous cycles. Performing more frequent measurements is desirable since they are likely to result in increased power output. However, this enhancement of output is accompanied by a nontrivial time evolution of the system that expresses itself through temporal correlations in the statistics of consecutive measurement outcomes. Such correlations make the thermodynamics of information engines both richer and harder to analyze. A recent theoretical paper discussed the role of correlations in a simple two-state system [18]. Here, we

offer an experimental realization of an information engine that naturally operates in a regime where correlations are important. Our experimental setup also has the appealing feature that it offers an almost clean conversion of information to work.

Our information engine resides in a glass chamber, 40 μm in height, filled with a dilute colloidal suspension of poly(2, 2, 3, 3, 4, 4, 4-heptafluorobutyl methacrylate) (PHM) colloidal particles ($d \sim 1$ μm, $n_p = 1.38$) [19] and an aqueous solution of 42% sucrose ($n_m = 1.42$). A repelling wall, made out of an array of 19×3 laser beams, focused to a diffraction limited spot by a 100x objective, with a total power of 0.3 W, is placed within the chamber near a colloidal particle [see Fig. 1(a)]. Relative flow is introduced by moving the sample with respect to the optical wall with constant velocity $v = 0.100$ μm/s using an XY nanopositioning system (PI-542.2CD). The optical wall is created and displaced using a holographic optical tweezers (HOT) setup [21,22]. Optical repulsion of the colloid from the light wall is achieved by ensuring $n_p < n_m$. Therefore, the light blocks the motion of the colloidal particle, but not that of the fluid.

A colloidal particle placed in the channel will execute a biased Brownian motion caused by the drag force applied on it by the fluid, $\vec{F} = -\gamma\vec{v}$, with $\gamma = 6\pi\eta a$, where η is the suspension viscosity and a the particle radius. When the particle is near the barrier, it feels an additional force due to the effective repulsion of the laser light. Let us denote the particle's distance from the center of the barrier by Δx. A one-dimensional approximation for the potential felt by the particle is [Fig. 1(b)],

$$U_{\text{eff}}(\Delta x) = U_{\text{op}}(\Delta x) + U_f(\Delta x) = A\exp^{-(\Delta x)^2/2\sigma^2} + \gamma v \Delta x, \quad (2)$$

where U_{op} is the optical potential created by the HOT, U_f is the effective potential arising from the fluid drag force, and A and σ denote the magnitude and width of the optical barrier.

If left alone, the colloidal particle will relax to an equilibriumlike state in this effective potential. To create an information engine, we periodically measure the particle location and move the barrier upstream when the particle is found to be far enough from the barrier. Specifically, we pick a distance Δx_0, which is located in the linear part of the potential, and divide the region of $\Delta x > \Delta x_0$ into cells of size $\delta = 0.21$ μm. This value of δ ensures almost error free measurements [23]. Those cells correspond to the possible outcomes of measurements of the particle's position. For instance, $\Delta x_0 + (j-1)\delta \le \Delta x \le \Delta x_0 + j\delta$ is said to be in cell j. All points with $\Delta x < \Delta x_0$ are said to be in cell 0. If the particle is measured to be in cell $j \neq 0$, then the barrier is moved upstream $x_b(t^-) \to x_b(t^-) + j\delta$. No action is taken when the particle is found in cell 0. [See Fig. 2(a) for a heuristic depiction of the feedback protocol.] This operating mechanism is that of an information engine. When applied, the system will settle into a steady state in which the particle moves upstream by feedback steps that rectify thermal fluctuations. Similar models were studied theoretically in Refs. [24,25]. The former used a simplified discrete model with a hard wall that allowed for the calculation of thermodynamic quantities. The latter argued that maximum output requires using both information and direct work.

We use conventional video microscopy [26] to track the particle's motion with a precision of approximately 12 nm.

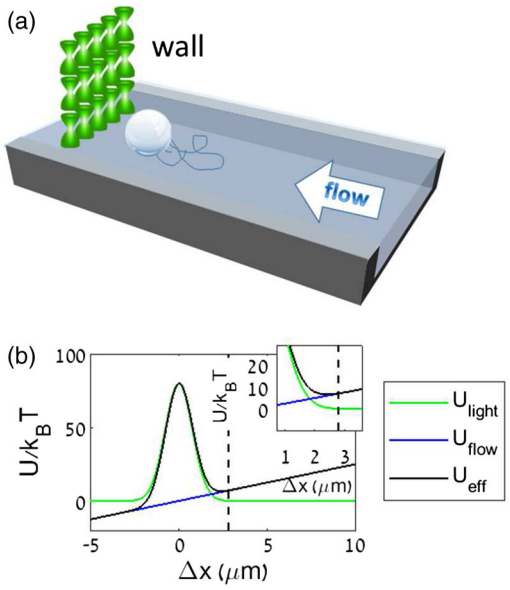

FIG. 1. (a) A particle driven by flow against a wall is tracked as it diffuses. Whenever the particle diffuses upstream, beyond a given threshold distance, the wall is moved closer to the particle. This measurement and feedback loop is repeated during the operation of the machine. (b) The effective potential that the particle experiences (black) is the sum of repulsion from the optical wall (green) and friction force from the flowing liquid (blue). The dashed vertical line indicates the threshold distance above which the wall is moved.

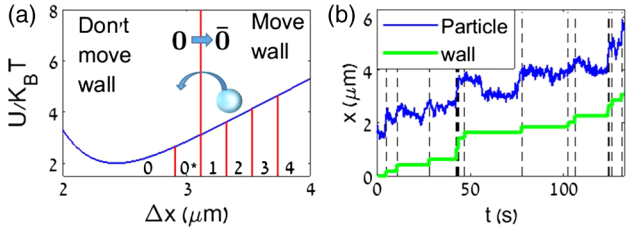

FIG. 2. (a) The potential landscape as a function of distance from the wall is divided into cells of size δ. When the particle crosses the threshold Δx_0, the wall is moved towards the particle, to place it within cell 0*. (b) Typical trajectory of a particle (blue line) and wall (green line) in a working information machine. Dashed lines highlight the wall movements.

From the particle's motion under a stationary barrier, we extract the effective one-dimensional potential acting on the colloidal particle and its diffusion coefficient (see [23] for details).

Figure 2(b) depicts a typical trajectory of the particle and the wall during the machine operation. In the Supplemental Material we show a movie of an operating machine. A trace of the trajectory of the particle is overlayed on the movie (blue), while the position of the light wall is indicated by a green line. When the feedback is on, the particle gradually moves against the flow (from left to right). When the laser is turned off the particle is no longer confined and is carried away by the flow in a relatively straight line.

Three important quantities characterize the thermodynamics of the information engine. The useful gained work in our setup is due to the upstream motion of the colloidal particle

$$W_{\mathrm{out}}(x(t)) = \gamma v(x(t_f) - x(t_i)), \tag{3}$$

where t_i and t_f stand for the starting and ending time of the experiment, respectively. Work is also done on the colloidal particle (i.e., the system) when the barrier is moved, since the potential landscape in which the particle is moving is modified externally. This work is given by

$$W_{\mathrm{in}}(x(t)) = \sum_k U_{\mathrm{op.}}[x(t_k) - (x_b(t_k) + j_k\delta)] - U_{\mathrm{op.}}[x(t_k) - x_b(t_k)], \tag{4}$$

where t_k and j_k are the measurement times and outcomes corresponding to barrier motion. The last quantity, characterizing the Maxwell demon, is the amount of information acquired by measurements. For reasonably sized cells, we can neglect measurement errors, as is done, e.g., in Szilárd engine. For error free measurements, the Shannon entropy,

$$S_N = -\sum_{m_1,\ldots,m_N} P(m_N, m_{N-1}\ldots m_1)\ln P(m_N, m_{N-1}\ldots m_1), \tag{5}$$

characterizes the mean information gained from a series of N measurements (with outcomes $m_1, \ldots, m_N$).

An important feature of our experimental setup is the appearance of correlations between outcomes of consecutive measurements. Our system exhibits dynamics with two typical time scales. τ_{MFP} is the mean time it takes the particle to reach the threshold for barrier motion for the first time after the barrier was moved (i.e., the mean first passage time). τ_{rel} is the time scale for the relaxation of the probability distribution to a quasiequilibrium state with a complete loss of temporal correlations. In our experiments, $\tau_{\mathrm{MFP}} \simeq 1$ s and $\tau_{\mathrm{rel}} \simeq 30$ s. These time scales should be compared to the time between consecutive measurements Δt. $\Delta t > \tau_{\mathrm{rel}}$ means that the correlations between measurements are negligible. This regime is easy to analyze, and it was studied in many experimental realizations of information engines. Reducing Δt leads to increased power output, accompanied by correlations between measurements. We therefore performed our experiments for several values of Δt in the range 0.14–50 s.

At steady state, the system can be characterized by the mean rate of accumulation of work and information. Among these, the hardest to estimate is the mean rate of information growth, $\dot{I}_{\mathrm{ss}} \equiv \lim_{N\to\infty} S_N/N\Delta t$. Direct calculation of the Shannon entropy in Eq. (5) is unrealistic since it is exceedingly hard to gather enough statistics to deduce the probability distribution $P(m_N, m_{N-1}\ldots m_1)$ with any degree of accuracy. Nevertheless, our choice of feedback protocol allows for an approximation, which takes into account most of the relevant correlations. Consider the conditional probability describing the evolution after motion of the barrier. By design, the barrier is moved so that the particle is placed in cell 0^* [indicated in Fig. 2(a)]. This means that the probability distribution that serves as the initial condition for subsequent evolution is nonvanishing only in a small cell of size δ. We assume that the small variation of position within cell 0^* can be neglected, which means that to a good approximation, correlations are lost following barrier motion, a fact that can be expressed mathematically as $P(m_i|m_{i-1} \neq 0, m_{i-2}, \ldots) \simeq P(m_i|\bar{0})$. $\bar{0}$ is a shorthand for $m \neq 0$. We stress that this observation does not mean that all correlations are lost. Correlations can and do persist when the outcome of a measurement is 0, and the barrier is not moved. This approximation improves when δ becomes smaller.

With the help of this approximation, the rate at which information is acquired at a steady state can be recast as

$$\dot{I}_{\mathrm{ss}} \simeq -\frac{1}{\Delta t}\sum_{m,m'\neq 0}[P(m', m)\ln P(m'|\bar{0}) + P(m', 0, m)\ln P(m', 0|\bar{0}) + P(m', 0, 0, m)\ln P(m', 0, 0|\bar{0}) + \cdots], \tag{6}$$

where, for instance, $P(m', 0, 0, m)$ is the probability of a sequence of measurements in which the particle is found in cell m, then found in cell 0 twice in a row, and finally is found in m'. An estimation of Eq. (6) is considerably easier than that of Eq. (5) since it is built from much shorter segments of outcomes that are easier to sample. The series in Eq. (6) converges since the probability to not move the barrier is expected to decrease for $t > \tau_{\mathrm{MFP}}$, leading to smaller and smaller terms. Figure S3 [27] shows the convergence of information for a different Δt; 40 terms are needed to estimate $\dot{I}_{\mathrm{ss}}$ for $\Delta t = 200$ s, while 600 terms are required for $\Delta t = 0.14$ s. While an estimation of the rate of acquisition of information using Eq. (6) is not as prohibitive as one based on Eq. (5), it was still impossible

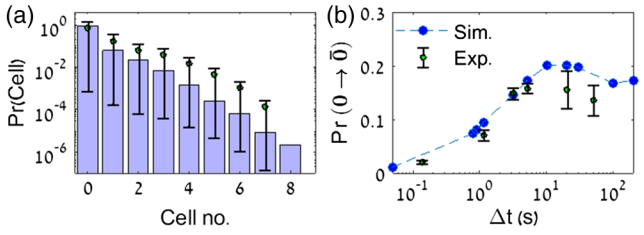

FIG. 3. (a) Probability distribution of cell occupation from experiment (green circles) and simulation (blue bars) at $\Delta t = 3$ s. The occupational probability decays exponentially with the distance from the optical barrier. (b) The probability of consecutive 0 and $\bar{0}$ measurements, $Pr(0 \to \bar{0})$. Namely, the probability of events where the particle was found close to the barrier but was found to be far from the barrier in the consecutive measurement.

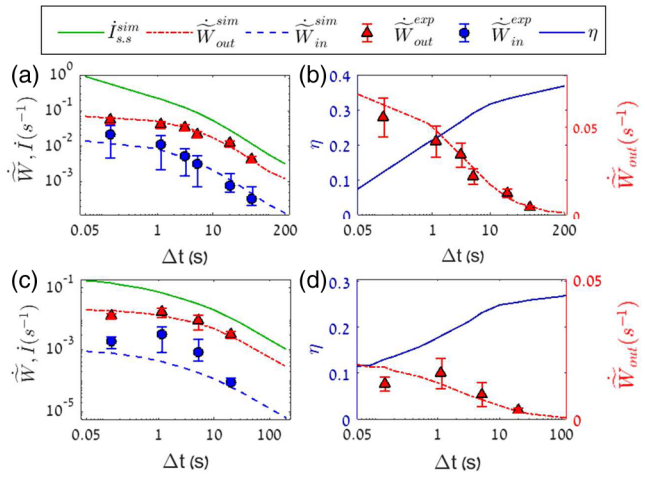

FIG. 4. (a),(c) Comparison between normalized output power $\dot{\tilde{W}}_{\rm out} = \langle \dot{W}_{\rm out} \rangle / k_B T$, direct input power $\dot{\tilde{W}}_{\rm in} = \langle \dot{W}_{\rm in} \rangle / k_B T$, and the information rate $\dot{I}_{\rm ss}$ as a function of time between measurements for $\Delta x_0 = 2.77$ μm (a), and $\Delta x_0 = 3.12$ μm (c). (b),(d) Comparison between efficiency η and normalized output power $\dot{\tilde{W}}_{\rm out}$ as a function of time between measurements for $\Delta x_0 = 2.77$ μm (a), and $\Delta x_0 = 3.12$ μm (c). Simulation results are presented in lines, while experimental results are presented in symbols.

to repeat our experiment enough times to obtain a reliable estimate of $\dot{I}_{\rm ss}$. Instead, we have used numerical simulations (Langevin dynamics [28]) to calculate this quantity. To ensure that the simulations represent the experiments well, we used the same effective potential and temperature. We also compared the simulated probability distribution to be in a given cell $P(\text{cell})$ to its experimentally measured counterpart [Fig. 3(a)], and we find good agreement between experiment and simulation probability distributions. The experimental probabilities are slightly higher than the numerically calculated probabilities due to the undercounting of rare events, such as the occupation of cell 8. Figure 3(b) compares measurements and simulations of the probability to find the particle in cell 0, and in the following measurement, find it with $\Delta x > \Delta x_0$. Good agreement is found. In Fig. 3(b), a lack of statistics prevents the convergence of $Pr(0 \to \bar{0})$ at large Δt. Our simulations therefore reasonably reproduce both single and two-measurement quantities.

A fingerprint of the temporal correlations taking place at high frequency measurements is seen in the probability distribution of the first passage time (FPT), i.e., the time it takes the particle to reach $\Delta x > \Delta x_0$ for the first time since the barrier was moved. In Fig. S5 [29], the simulated FPT distribution is plotted for different values of Δt. For a small Δt, the FPT distributions exhibit a small peak followed by an exponential decay. Only the exponential part is observed for larger values of Δt. We believe that this peak represents occasions in which the particle makes a thermal fluctuation upstream right after the barrier was moved. Such events will be less likely to be observed for a larger Δt. We expect, therefore, that short intervals between measurements will allow the machine to take advantage of the peak in the FPT distribution, resulting in increased output power.

We now turn to study the thermodynamics of our information machine. We define the output power of the machine as:

$$\dot{W}_{\rm out} = \langle W_{\rm out}(x(t)) \rangle / \tau, \tag{7}$$

where $\tau = t_f - t_i$ is the duration of a whole experiment and $\langle \cdots \rangle$ denotes average over experimental realizations. In Fig. 4(a) and Fig. 4(c), $\langle \dot{W}_{\rm in} \rangle$, $\langle \dot{W}_{\rm out} \rangle$, and $\dot{I}_{\rm ss}$ are shown as a function of Δt for $\Delta x_0 = 2.77$ μm and $\Delta x_0 = 3.12$ μm, respectively. The probability distributions of the work rate were found to be Gaussian [30]. Here, $\dot{I}_{\rm ss}$ is the mean information gain per unit time, calculated from Eq. (6) with the help of computer simulations. Clearly, both work and information gain per unit time decrease as $1/\Delta t$ for $\Delta t \geq \tau_{\rm rel}$. As Δt becomes smaller, $\dot{I}_{\rm ss}$ increases faster then the power output [Fig. 4(a)]. We ascribe this behavior to the fact that for $\Delta t \ll$ MFPT, the main increase in output power is due to the more immediate recognition of events of $\Delta x > \Delta x_0$, which only marginally increases the output power. Following [25], we define the efficiency of our information engine as:

$$\eta = \frac{\langle \dot{W}_{\rm out} \rangle}{\langle \dot{W}_{\rm in} \rangle + k_B T \dot{I}_{\rm ss}}. \tag{8}$$

In Fig. 4(b), both the efficiency and output power are plotted as a function of time between measurements. We find that the maximum power is obtained in the limit of frequent measurements, as expected since frequent detection allows us to move the barrier more often. We also find that the efficiency saturates at quasistatic conditions. The efficiency of our machine at the quasistatic limit is $\eta_{\rm max} = 37\%$ for $\Delta x_0 = 2.77$ μm [Fig. 4(b)] and $\eta_{\rm max} = 26\%$ for $\Delta x_0 = 3.12$ μm [Fig. 4(d)]. This value is slightly

higher than previously reported values for information engines [11].

The ratio of direct mechanical work applied on our system to the gained work extracted by the engine is in the range of 11%–20% according to our simulations and from 6%–58% in our experiments for $\Delta x_0 = 2.77\ \mu$m. For $\Delta x_0 = 3.12\ \mu$m, it's range is 0.4%–5% in simulation and 3%–19% in our experiments. Crucially, this ratio can be tuned by changing Δx_0. For large values of Δx_0, the information engine shows an almost clean conversion of information to work, but this is accompanied with decreased output power.

In conclusion, we have realized experimentally an information engine that almost exclusively converts information to work. Importantly, our information engine works at a regime in which correlations between measurement outcomes can not be ignored. We have estimated these correlations using a combination of analytical approximations, Eq. (6), and simulations. Our results show that this information engine exhibits a trade off between power output and efficiency that is commonly observed in heat engines, molecular motors, and other types of nanoscale machines. The existence of this trade-off suggests that choosing $\Delta t \simeq \tau_{\mathrm{MFP}}$ will balance between the desire to have high output power and efficiency.

Our highly flexible and almost pure information machine offers the possibility to study experimentally several new aspects of information engines. For example, the relation between the efficiency and output power, or the amount of information collected at each step and its dependence on the size of cells, δ. Another interesting topic is the effect of a feedback delay time between measurement and the application of the feedback on the engine characteristics. In a recent paper [25], it was suggested that maximization of output power is obtained when both direct work and information are used. Our setup allows us to study this by placing the threshold Δx_0 on the slope of the Gaussian barrier. Finally, more elaborate feedback protocols with memory can be investigated. These would employ past measurements to determine when and how much to move the barrier.

This research has been supported by the Israel Science Foundation (Grants No. 988/17 and No. 1526/15), and by the U.S.-Israel Binational Science Foundation (Grant No. 2014405).

*rahavs@ch.technion.ac.il
†roichman@tauex.tau.ac.il

[1] J. C. Maxwell, *Theory of Heat* (Appleton, London, 1871).
[2] K. Maruyama, F. Nori, and V. Vedral, Rev. Mod. Phys. **81**, 1 (2009).
[3] L. Szilard, Z. Phys. **53**, 840 (1929).
[4] C. E. Shannon, Bell Syst. Tech. J. **27**, 379 (1948).
[5] T. Sagawa and M. Ueda, Phys. Rev. Lett. **100**, 080403 (2008).
[6] T. Sagawa and M. Ueda, Phys. Rev. Lett. **104**, 090602 (2010).
[7] M. Ponmurugan, Phys. Rev. E **82**, 031129 (2010).
[8] J. M. Horowitz and S. Vaikuntanathan, Phys. Rev. E **82**, 061120 (2010).
[9] A. Bérut, A. Arakelyan, A. Petrosyan, S. Ciliberto, R. Dillenschneider, and E. Lutz, Nature (London) **483**, 187 (2012).
[10] Y. Jun, M. Gavrilov, and J. Bechhoefer, Phys. Rev. Lett. **113**, 190601 (2014).
[11] S. Toyabe, T. Sagawa, M. Ueda, E. Muneyuki, and M. Sano, Nat. Phys. **6**, 988 (2010).
[12] J. V. Koski, V. F. Maisi, T. Sagawa, and J. P. Pekola, Phys. Rev. Lett. **113**, 030601 (2014).
[13] J. V. Koski, V. F. Maisi, J. P. Pekola, and D. V. Averin, Proc. Natl. Acad. Sci. U.S.A. **111**, 13786 (2014).
[14] É. Roldán, I. A. Martínez, J. M. R. Parrondo, and D. Petrov, Nat. Phys. **10**, 457 (2014).
[15] A. Ruschhaupt, J. G. Muga, and M. G. Raizen, J. Phys. B **39**, 3833 (2006).
[16] J. M. R. Parrondo, J. M. Horowitz, and T. Sagawa, Nat. Phys. **11**, 131 (2015).
[17] M. D. Vidrighin, O. Dahlsten, M. Barbieri, M. S. Kim, V. Vedral, and I. A. Walmsley, Phys. Rev. Lett. **116**, 050401 (2016).
[18] M. Bauer, A. C. Barato, and U. Seifert, J. Stat. Mech. (2014) P09010.
[19] See Supplemental Material at http://link.aps.org/supplemental/10.1103/PhysRevLett.121.180601 for the colloidal synthesis details, which includes Ref. [20].
[20] G. H. Koenderink, S. Sacanna, C. Pathmamanoharan, M. Rasa, and A. P. Philipse, Langmuir **17**, 6086 (2001).
[21] D. G. Grier and Y. Roichman, Appl. Opt. **45**, 880 (2006).
[22] H. Nagar and Y. Roichman, Phys. Rev. E **90**, 042302 (2014).
[23] See Supplemental Material at http://link.aps.org/supplemental/10.1103/PhysRevLett.121.180601 for the potential energy characterization and cell size.
[24] F. J. Cao and M. Feito, Phys. Rev. E **79**, 041118 (2009).
[25] R. K. Schmitt, J. M. R. Parrondo, H. Linke, and J. Johansson, New J. Phys. **17**, 065011 (2015).
[26] J. Crocker and D. G. Grier, J. Colloid Interface Sci. **179**, 298 (1996).
[27] See Supplemental Material at http://link.aps.org/supplemental/10.1103/PhysRevLett.121.180601 for a study of the information calculation convergence.
[28] N. Grønbech-Jensen and O. Farago, Mol. Phys. **111**, 983 (2013).
[29] See Supplemental Material at http://link.aps.org/supplemental/10.1103/PhysRevLett.121.180601 for a study of FPT.
[30] See Supplemental Material at http://link.aps.org/supplemental/10.1103/PhysRevLett.121.180601 for a study of the distribution of W_{in} and W_{out}.